Long-Distance Altimetry and Terrain Relative Navigation Capabilities of a Multi-Functional Imaging Lidar for Precision Safe Landing

Farzin Amzajerdian[*], Aram Gragossian [†], Paul F. Brewster[‡], Jacob M. Heppler[§], Frederick G. Wilson[**], Mitchell J. Davis[††], Glenn D. Hines[‡‡], and Daniel K. Litton[§§]
NASA Langley Research Center, Hampton, VA 23681, USA

Alexander Bulyshev [***]
Coherent Applications Inc, Hampton, VA 23681, USA

A linear-mode flash lidar sensor employing a resolution enhancement algorithm is being developed at NASA Langley Research Center for enabling precise and safe landing on the Moon, Mars, and other destinations in the solar system. This lidar, referred to as Terrain Sensing Lidar (TSL), is a multi-mode sensor capable of hazard detection and avoidance, terrain relative navigation, and long-distance altimetry. TSL offers a solution for future missions that require landing in rough terrain and/or poor lighting conditions. The viability of TSL for terrain hazard detection and avoidance has already been demonstrated by conducting drone and helicopter flight tests. An upgraded version of this lidar has been recently assembled for additional aircraft flight tests to demonstrate its multi-mode capability including long-distance altimetry and terrain relative navigation.

I. Introduction

A 3-D imaging flash lidar sensor is being developed at NASA Langley Research Center for providing onboard ground-relative position knowledge and hazard avoidance capabilities to aid missions that require landing in rough terrain and/or poor lighting conditions. The main advantage of flash lidar technology over more conventional scanning lidar is the ability to record full 3-D images with a single laser pulse, freezing the scene on every frame by removing all motion of the transmitter/receiver platform [1,2]. Linear-mode flash lidar records the 3-D image frames at a high rate by imaging the illuminated scene onto a Focal Plane Array (FPA). Each pixel in the FPA takes independent measurements of the lidar pulse time of flight to the target. Therefore, the flash lidar does not require position and attitude angle data from external sensors and extensive computation resources and time for compensating vehicle motion during image acquisition. Another advantage is having uniformly distributed pixels

[*] Principle Investigator, LaRC Remote Sensing Branch, Engineering Directorate.
[†] System Development Lead, LaRC Remote Sensing Branch, Engineering Directorate.
[‡] SW Lead, LaRC Flight Software Branch, Engineering Directorate.
[§] M.E. Lead, LaRC Mechanical Systems Branch, Engineering Directorate.
[**] E-O Lead, LaRC Remote Sensing Branch, Engineering Directorate.
[††] E-O Lead, LaRC Electronic Systems Branch, Engineering Directorate.
[‡‡] Chief Engineer, Engineering Directorate.
[§§] Project Manager, Space Technology and Exploration Directorate.
[***] Algorithms Lead and System Analyst, LaRC Remote Sensing Branch, Engineering Directorate.

with each image frame which simplifies the hazard detection algorithm and reduces the risk of false alarms. Furthermore, its high frame rate allows for timely generation of 3-D maps of the landing area and subsequent selection of safe landing locations. Another important feature of flash lidar technology is the ability to perform other key functions during descent which are necessary for precision navigation towards an intended landing site. These essential functions are altimetry, Terrain Relative Navigation (TRN) [3], and Hazard Relative Navigation (HRN), in addition to Hazard Detection and Avoidance (HDA) [4,5].

The capabilities of this lidar, referred to as Terrain Sensing Lidar (TSL), for generation of digital elevation maps and detection of hazardous terrain features have already been demonstrated [6]. The work on TSL is now focused on evaluating its performance as a multi-functional sensor providing altitude and TRN data from high altitudes. Fig. 1 shows operation of our lidar sensor in the context of a lunar landing. For illustration purpose, it is assumed that the lidar is pointed nadir during the altimetry and TRN phase and pointed along the flight path at 45 degrees during the HDA phase. The lidar begins its operation after a deorbit maneuver at about 60 km above the ground. At this stage, the lidar transmitter beam is focused to illuminate only a few pixels in the center of the detector array to measure range to the ground. Reducing the divergence of the lidar transmitter beam to a fraction of its receiver field of view increases its operational slant range to ~60 km from a nominal 1.4 km. The ground-relative altitude measurements provided by TSL can reduce a spaceflight vehicle's position error significantly since it is normally derived from an Inertial Measurement Unit (IMU) which suffers from drastic drift over its travel time from Earth. The IMU drift error can be about 1 km for a Moon-bound vehicle and 10 km for Mars. Accurate altitude data reduces position error to a few hundred meters.

When the altitude drops to about 20 km, the TSL begins its TRN mode of operation in which the lidar beam is expanded to illuminate a section of the detector array encompassing more than hundred pixels. In this mode, the lidar illuminates a swath about 120 m wide and generates relatively low-resolution overlapping 3-D image frames along the flight path. These image frames are stitched together periodically to produce elevation maps that are subsequently compared with stored maps having known surface features such as craters. This TRN process further reduces the vehicle's relative position error from hundreds of meters to tens of meters.

From about 1 km to 0.5 km altitude, the TSL operates in the HDA mode with its full field of view, generating a high-resolution elevation map of the landing area. This elevation map is then processed to identify hazardous features such as rocks, craters, and steep slopes, and to determine the most suitable landing location. In the case of lunar landing, the flight trajectory angle is nominally around 45 degrees at 1 km altitude which makes the slant range to the ground about 1.4 km. TSL can update the elevation map multiple times before initiation of the pitch up maneuver in order to verify the selected landing location. TSL can continue acquiring 3-D image frames at video rates for performing the HRN function that uses terrain features as markers for continuous trajectory correction toward the selected landing location. Altitude data is provided continuously during the entire TSL operation from 60 km to several meters above the ground depending on the opacity of the engine-induced dust plume.

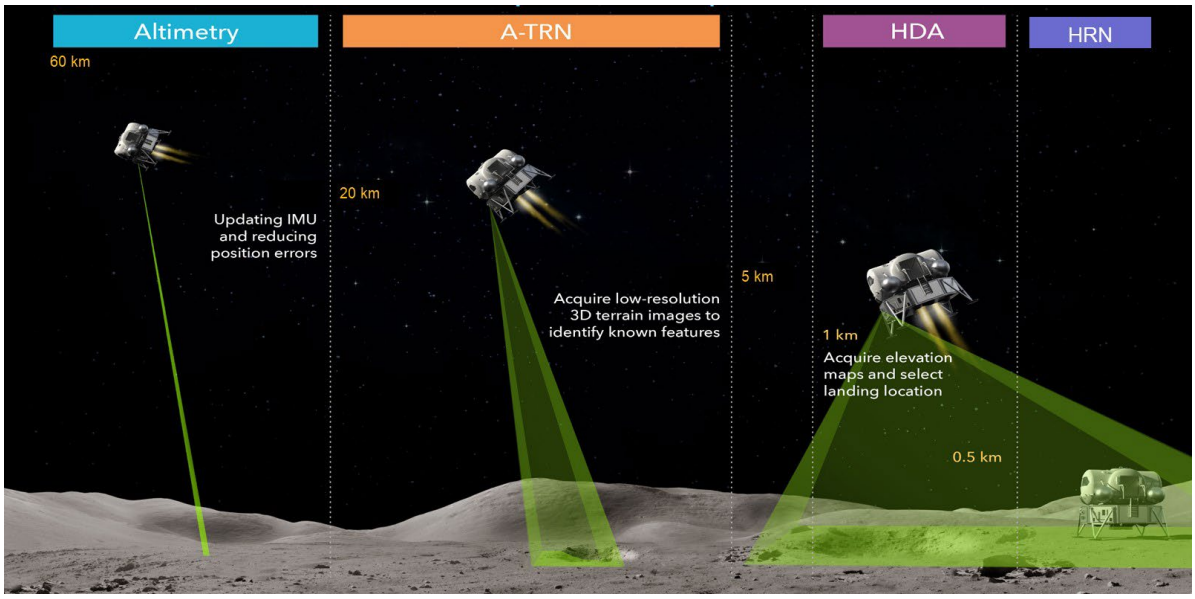


Figure 1. An operational concept of Terrain Sensing Lidar for lunar landing.

II. Terrain Sensing Lidar Brassboard

The performance of TSL for HDA has already been demonstrated by conducting drone and helicopter flight tests using a breadboard unit. The results of those flight tests were reported at the AIAA Scitech Forum last year [6]. Since then, a brassboard version of TSL has been built (Fig. 2) with an extended operational range of 1.4 km for HDA with the incorporation of multi-functional capability for performing long-distance altimetry and TRN. The brassboard unit weighs about 7 kg, consumes 43 W, and uses components with a clear path to space, providing a solid foundation for low-risk, low-cost, and timely production of spaceflight units.

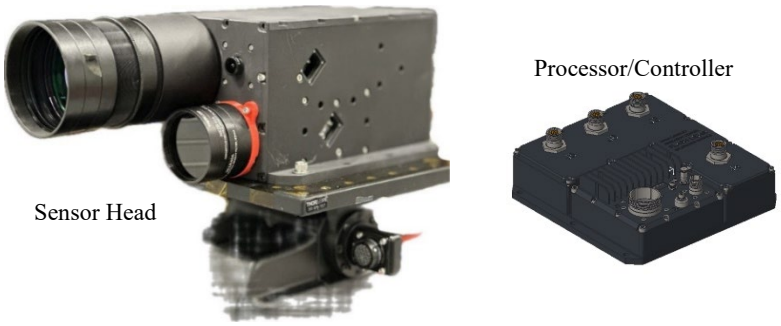


Figure 2. Terrain Sensing Lidar (TSL) brassboard with multi-functional capability.

The real-time image processing algorithms enable the TSL to operate as a standalone sensor without the need for position and attitude data from external sensors. Conversely, these same image-enhancement and processing algorithms also generate relative position, attitude, and vector-velocity data as a byproduct. Table 1 summarizes the projected performance of TSL in different modes of operation. TSL provides two primary data products: ground range measurements and Digital Elevation Maps (DEMs). These data products are readily integrated into the vehicle's flight computer to derive ground-relative altitude and position. The navigation filter fuses TSL range measurements with IMU data to compute altitude. Meanwhile, the TRN algorithm correlates TSL-generated DEMs with onboard terrain elevation maps to estimate the vehicle's position relative to the intended landing location or other relevant terrain features.

Table 1. TSL Brassboard Projected Performance Specifications.

Altimetry	
Operational Range	60 km – 2 m
Precision 1-σ	$0.08 + 2x10^{-5}xR$ m
Update Rate	20 Hz
Terrain Relative Navigation	
Operational Range	20 km – 5 km
Swath Width	120 m
Ground Sample Distance	6.8 m @ 10 km
Elevation Precision 1-σ	10 cm
Frame Overlap	30% @ 20 km, 60% @ 10 km
Hazard Detection and Avoidance	
Operational Range	1.4 km slanted path
Digital Elevation Map (DEM) Size	1.05M pixels
DEM Update Rate	1 Hz
Minimum Detectable Hazard	25 cm radius
Relative Navigation Data	
Operational Range	1.4 km
Position	15 cm
Attitude	0.05°
Velocity	20 cm/sec
Update Rate	20 Hz

In Altimetry mode, the TSL laser beam has a ground footprint on the order of tens of meters in diameter, depending on vehicle altitude. Consequently, terrain topography can introduce additional uncertainty into the range measurement. The precision values listed in Table 1 assume flat terrain; therefore, terrain-induced effects, together with beam-pointing jitter from vehicle vibrations, must be accounted for when estimating vehicle altitude.

In TRN mode, the TSL beam divergence is adjusted to cover an approximately 120-m swath along the flight path for much of its operational altitude range as shown in Fig. 3. A variation of the Super-Resolution (SR) algorithm that is used for HDA DEMs [7,8] is utilized for back-projecting and stitching 20 range image frames and generating a TRN DEM every 1 sec. The algorithm takes advantage of the image overlaps for stitching the image frames and improve the resolution in one axis along the flight path. Therefore, each DEM is about 120 m x 1000 m when traveling with 1000 m/sec horizontal velocity. The simulation of the TRN operation of the TSL has shown that position estimation of better than 1 m can be achieved at 10 km altitude. The Ground Sample Distance (GSD) varies with altitude resulting in a precision in position determination that is scaled with altitude.

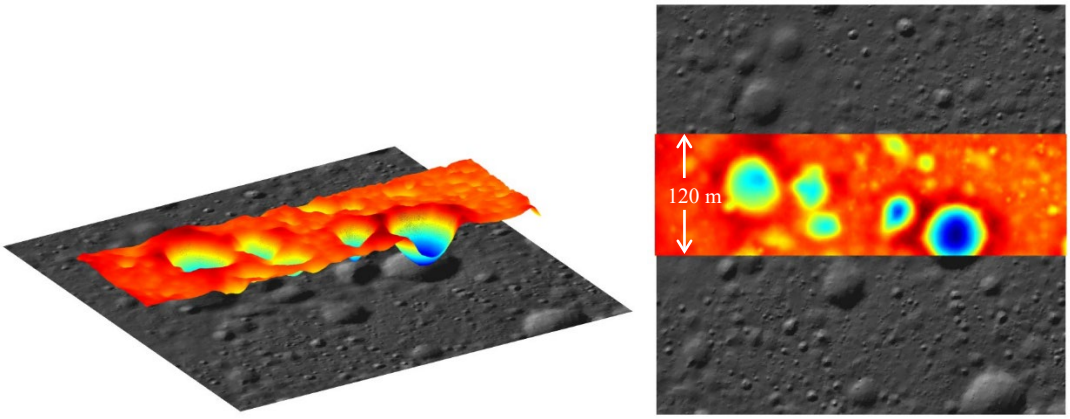


Figure 3. TSL generates DEMs of a continuous swath of the terrain along the flight path.

In HDA mode, the laser beam divergence is widened to match the receiver field-of-view thereby illuminating the full 16.4k-pixel array. As previously described [6–8], the real-time SR algorithm generates 1024×1024-pixel DEMs at a 1 Hz rate, enabling reliable detection of hazards with a 25-cm radius from slant ranges up to 1.4 km.

III. Future Work

Ongoing efforts focus on characterizing the TSL brassboard and implementing design refinements to enhance performance and operational robustness. Initial static tests at the NASA LaRC lidar test range, along with a drone-based flight test of the brassboard, have already been completed. Current work includes preparations for a high-altitude aircraft flight test scheduled for the Spring of 2026, aimed at demonstrating long-range altimetry and TRN operation of the TSL. This test will be conducted in California using the NASA AFRC's ER-2 aircraft, which can operate at altitudes up to 20 km above the ground. The campaign will provide an excellent evaluation of the TSL's capabilities and its ability to meet the performance specifications for each operational mode summarized in Table 1. The resulting data will inform further design and algorithm improvements and help pave the way toward developing spaceflight units suitable for a wide range of landing missions.

IV. Conclusion

A multi-functional lidar sensor based on linear-mode flash lidar technology, combined with novel image-enhancement and processing algorithms, has been developed to perform three key functions required for precise and safe landing. This sensor, known as the Terrain Sensing Lidar, can enables long-range altimetry, Terrain Relative Navigation, and Hazard Detection and Avoidance thus meeting the needs of future missions requiring precision safe landing at designated locations on the Moon or other destinations in the solar system under any lighting conditions. TSL operating at close to video rate can also be used for Hazard Relative Navigation, after completion of the hazard detection phase and selection of landing location, to further improve the precision and safety of a touchdown maneuver. A brassboard version of TSL has recently been completed and is being prepared for a high-altitude aircraft flight-test campaign. This campaign will serve as a stepping stone towards the development of spaceflight-ready units.

Acknowledgments

The authors are grateful to the Center Director's Office and the Space Technology and Exploration Directorate (STED) at NASA Langley Research Center for their continued support. The authors also gratefully acknowledge the longstanding support of Jeffrey Herath, STED Deputy Director, and Kevin Somervill, Deputy Director for NASA Technology Maturation at Space Technology Mission Directorate, for their continued confidence in our work.

References

[1] F. Amzajerdian, V. E. Roback, A. E. Bulyshev, P. F. Brewster, W. A. Carrion, D. F. Pierrottet, G. D. Hines, L. B. Petway, B. W. Barnes, and A. M. Noe, "Imaging flash lidar for safe landing on solar system bodies and spacecraft rendezvous and docking," Proc. SPIE Vol 9465, 2015.

[2] F. Amzajerdian, V. E. Roback, A. E. Bulyshev, P. F. Brewster, G. D. Hines, "Imaging Flash Lidar for Autonomous Safe Landing and Spacecraft Proximity Operation," AIAA SPACE Forum, 10.2514/6.2016-5591, 2016.

[3] A. E. Johnson, J. Montgomery, "An Overview of Terrain Relative Navigation for Precise Lunar Landing," IEEE Aerospace Conference, 2008.

[4] A. Huertas, A. E Johnson, R. A. Werner, R A. Maddock, "Performance Evaluation of Hazard Detection and Avoidance Algorithms for Safe Lunar Landings," Proc. IEEE Aerospace Conference, PP 1-20, 2010.

[5] V. E. Roback , D. F. Pierrottet, F. Amzajerdian, B. W. Barnes, G. D. Hines, L. B. Petway, P. F. Brewster, K. S. Kempton, and A. E. Bulyshev, "Lidar sensor performance in closed-loop flight testing of the Morpheus rocket-propelled lander to a lunar-like hazard field," Proc. of AIAA Science and Technology Forum and Exposition, 2015.

[6] F. Amzajerdian, A. Gragossian, A. E. Bulyshev, P. F. Brewster, J.M. Heppler, F.G. Wilson, G. D. Hines, S.A, Laughter, D.K. Litton, "Development of a Compact Lidar Sensor for Terrain Relative Navigation and Terrain Hazard Avoidance," AIAA SciTech, 2025

[7] A. E. Bulyshev and F. Amzajerdian, "Hazard Avoidance Algorithm for a 3-D Imaging Flash Lidar Utilizing Multi-Frame Super-Resolution Technique," AIAA Guidance, Navigation, and Control Conference, AIAA SciTech Forum, 2023.

[8] A. E. Bulyshev, F. Amzajerdian, V. E. Roback, G. Hines, D. Pierrottet, and R. Reisse, "Three-dimensional super-resolution: theory, modeling, and field test results," Appl. Opt. 53(12), 2583, 2014.